5-9-1995

Optical Microscopy and Atomic Force Microscopy Imaging of 2,4,6-Trinitrotoluene Droplets and Clusters on Mica

D. O. Henderson
Fisk University

M. A. George
Fisk University

A. Burger
Fisk University

R. Mu
Fisk University

Zhiyu Hu
Fisk University

See next page for additional authors

Follow this and additional works at: https://digitalcommons.usu.edu/microscopy

Recommended Citation

Utah State University
MERRILL-CAZIER LIBRARY

Optical Microscopy and Atomic Force Microscopy Imaging of 2,4,6-Trinitrotoluene Droplets and Clusters on Mica

Authors

D. O. Henderson, M. A. George, A. Burger, R. Mu, Zhiyu Hu, and G. C. Huston

OPTICAL MICROSCOPY AND ATOMIC FORCE MICROSCOPY IMAGING OF 2,4,6-TRINITROTOLUENE DROPLETS AND CLUSTERS ON MICA

D.O. Henderson[*], M.A. George, A. Burger, R. Mu, Zhiyu Hu, and G.C. Huston[1]

Physics Department, Fisk University, Nashville, TN 37208
[1]Federal Aviation Technical Center, Atlantic City International Airport, Atlantic City, NJ 08405

Abstract

Optical and atomic force microscopy (AFM) were used to image 2,4,6-trinitrotoluene (TNT) on a cleaved mica (001) surface. The vapor deposition of TNT resulted in ellipsoidal drop formation on the mica surface. The growth rate of the drop diameter was found to be linear with vapor dosing time while the drop density followed a $1/r^2$ dependence, where r is the length of the major axis of the ellipsoid, for increasing dosing times. TNT platelets surrounded by a region depleted of drops were observed after 8 hours of dosing. The depleted region is attributed to a 10% shrinkage for liquid-solid transition for TNT and also from the enthalpy of fusion which causes the vaporization of small drops and clusters of TNT. Residues of TNT located in the depleted regions were characterized by AFM lift-off forces and were attributed to different morphologies of TNT that nucleated at different sites on the mica surface or dinitro- and trinitro-benzene derivatives which are common impurities in 2,4,6-trinitrotoluene.

[*]Address for Correspondence
D.O. Henderson
Fisk University
Nashville, TN 37208

Telephone number: (615) 329-8622
FAX number: (615) 329-8634

Introduction

The detection of explosive materials is of great interest to national security. Recently there have been significant efforts aimed at developing explosive vapor detection systems (Khan, 1992). In all vapor detection systems, it is necessary to preconcentrate the explosive materials on a surface and later release them for detection. The preconcentration of explosives on a surface is therefore the first step in explosives detection. The transport of atmosphere containing explosive vapors to a preconcentrator surface can lead to losses of explosives by adsorption on the transport line surfaces. Due to the intrinsically low vapor pressures of most explosives (Leggett, 1977; Pella, 1977) losses by adsorption can be significant and therefore can degrade the efficiency of an explosives detection system. Although references to explosives losses by adsorption have been reported previously (Henderson *et al.*, 1993), no studies have focused on characterizing the morphology of explosives adsorbed on surfaces. As a first step in characterizing explosive vapor adsorption on surfaces, we have imaged by optical microscopy and atomic force microscopy (AFM), 2,4,6-trinitrotoluene (TNT) adsorbed on a freshly cleaved mica surface.

Experimental

TNT was deposited on the (001) face of the mica substrates by vapor dosing. The deposition of the vapor was controlled by varying the temperature of TNT and the dosing time. The mica substrate was maintained at 298 K during deposition and the source TNT was heated to 398 K. The amount of TNT delivered to the mica surface by vapor deposition is difficult to determine accurately as there is significant scatter in the vapor pressure data reported by various investigators (Leggett, 1977; Pella, 1977). However, we estimate that at 398 K, the emission rate of TNT at equilibrium is $\sim 10^{19}$ molecules $cm^{-2} \cdot s^{-1}$. Under these conditions, and assuming a sticking coefficient of 1 for TNT on mica, a dosing time of 1 second should produce 1-2 monolayers
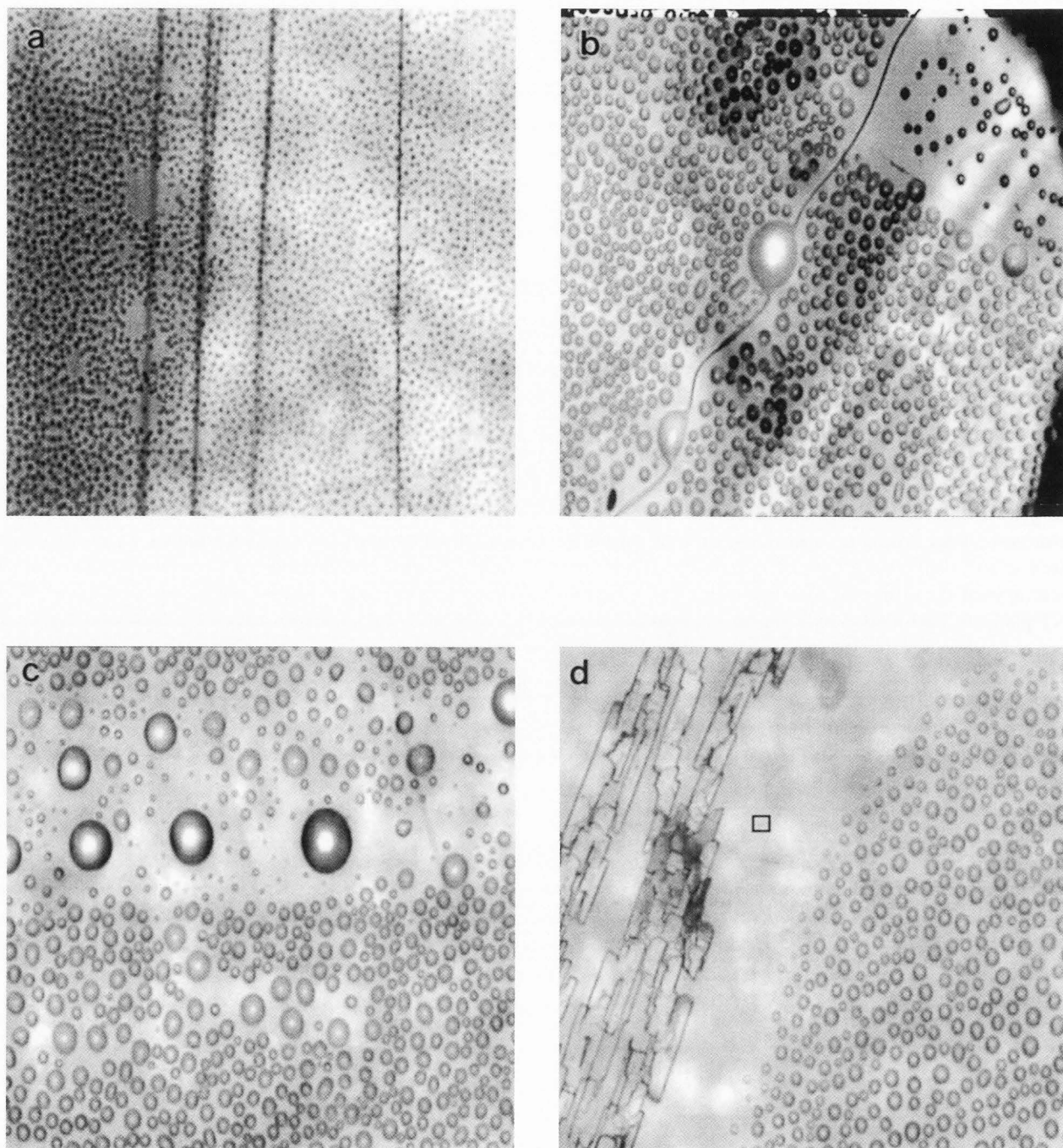
Figure 1. Optical micrographs for mica dosed with TNT for (a) 1 hour, (b) 4 hours, (c) 6 hours and (d) 8 hours; framed region is area imaged by AFM.

---

of TNT. Typically, we used dosing times between 15-360 minutes. The mica surfaces deposited with TNT were imaged by atomic force microscopy using a commercially available instrument (Nanoscope II, Digital Instruments, Santa Barbara). The scanning tips were Si_3N_4 cantilevers, 200 μm long and with a manu-

facturer-quoted spring constant of 0.12 N/m. All images were obtained in the constant force mode under ambient conditions, with a relative humidity between 50-70%. The images as presented in this paper were raw data. The optical microscopy was carried out using a Digital Optizoom microscope.
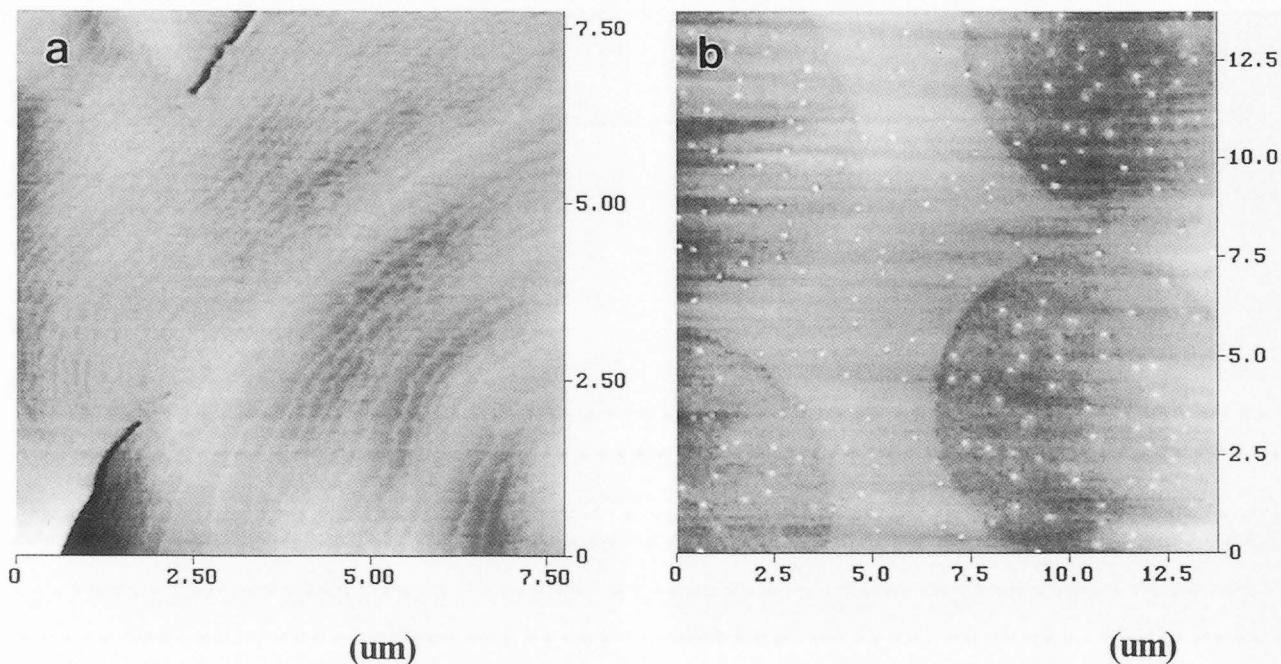
Figure 2. AFM of a sample dosed with TNT for 8 hours. In (a) the surface of a TNT crystallite that nucleated and grew on the surface of the mica substrate was imaged (z-range for the image is 100 nm). The region between the droplets and the crystallites was imaged in (b) (shown as the framed region in Figure 1d)

Results

Figures 1a, 1b, 1c, and 1d show the optical micrographs of TNT dosed on the (001) face of mica. The images clearly reveal that TNT is collecting on the mica surface as droplets. As the dosing time increases, the mean size of the droplet (determined from the length of the major axis of the ellipsoid or the diameter if the droplet is spheroidal) also increases and the density of droplets decreases. After a dosing period of $t \geq 4$ hours, the drops appear slightly ellipsoidal, and they show a preferred orientation with the major and minor axes of the individual drops aligned parallel to each other. At a dosing time of 4 hours, the mean droplet size is 3.3 μm; however large drops have grown along a defect as indicated in Figure 1b. Figure 1c shows an increase in the drop size after 6 hours of dosing. At this stage, the ellipsoidal shape and orientation of the major and minor axes are more clearly revealed. Several large drops have also developed with the major axes ranging between 47-66 μm. The regions where larger drops are observed are surrounded by zones depleted of the smaller drops. Figure 1d shows that after 8 hours of dosing the substrate, crystallites of TNT appear on the surface. The crystals grew faster in one direction, as is evident from the long parallel platelets shown in the figure which is typical of the morphology of TNT crystals

grown from the melt (Philp and Thorpe, 1976). There is also a region ~ 120 μm in diameter surrounding the crystallites where no drops are observed. However, at distances greater than 120 μm, relatively small 6 μm drops are observed, and at greater distances, the mean drop size increases.

Figure 2 depicts AFM images of a sample of mica dosed for 8 hours with vapors from the TNT source heated to 400 K. Figure 2a was obtained on the TNT crystallites and Figure 2b is in the region close to where the crystallization occurred in the depleted area (the box on Figure 1d). The AFM images obtained on the crystallites (shown in Figure 2a) resembled AFM images from the surface of TNT single crystals grown from solution. For the images obtained off the crystallites, two distinct features are apparent in the 12 x 12 μm scan (as shown in figure 2b): negative contrast circles varying in size from 6-10 μm in diameter and about 50 nm deep, as well as much smaller positive contrast features that are approximately 150 nm in diameter and 10-15 nm high. A closer examination of the smaller positive features is shown in Figure 3a. Repeated scanning in the same area reveals that these features are rigid, and not moved or modified by the cantilever tip. However, when the regions between the light features were scanned, obvious tip-induced surface modifications were apparent as can be seen in Figure 3b. When the scan
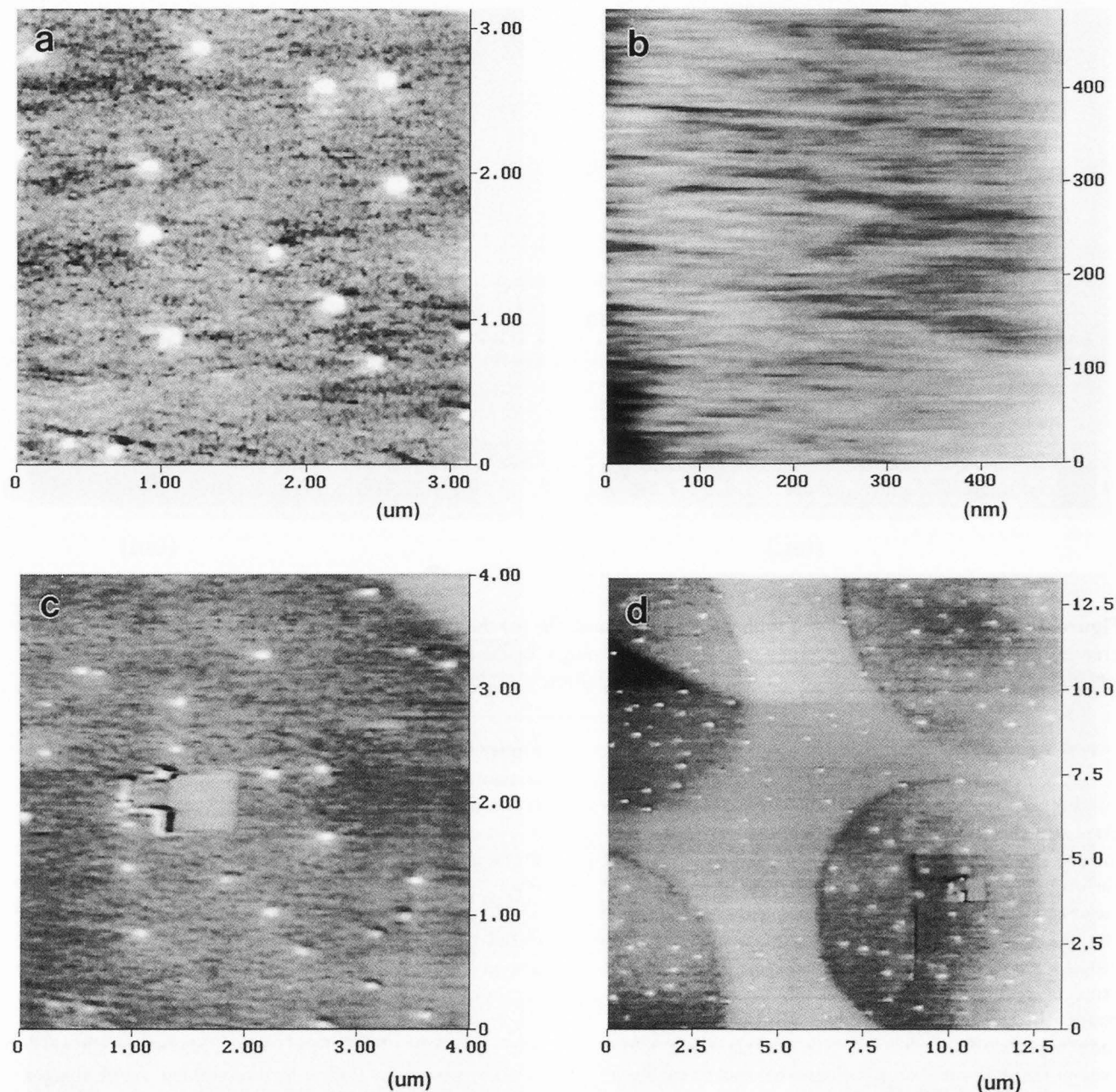
389

Figure 3. Atomic force microscopy images of the depleted area where nucleation occurred for the sample dosed 8 hours (z range for the images is 100 nm). A 13 x 13 μm scan shows (a) where both bright, sharp features as well as the large circular regions can be seen. In (b), a 3 x 3 μm scan is shown obtained from within one of the large circular regions. When a still smaller scan is made in this region, the surface appears to be distorted as shown in (c). In (d), a 4 x 4 μm scan reveals the region that was previously scanned in 3c indicating removal of material.

size was increased, the area that was previously scanned can be seen as a scraped-out region (shown in Figure 2d). Increasing the scan size again (Figure 3d) reveals the region of these overlapping scans produced by the cantilever tip.

In order to examine the variation of the adhesion forces between the tip and the sample at different re-

gions on the TNT coated mica, the liftoff forces were determined for several samples and ranged between 25-30 nN in regions outside of the TNT induced circular features, and 60-75 nN within the circle. These values were calculated using the manufacturer-quoted spring constant of 0.12 N/m, and as such cannot be taken as absolute measures of the liftoff forces, but as relative
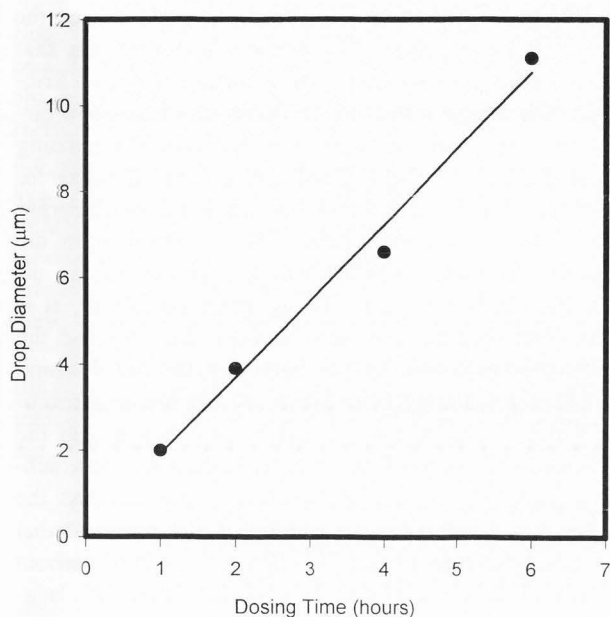
Figure 4. Mean drop diameter dependence on the dosing time.

----

values in the different regions on the sample.

Discussion

TNT has a melting transition at 353 K and is known to supercool to 300 K (Federoff, 1980). Thus it is not surprising that TNT adsorbed on mica is observed as a liquid at ambient temperature where our measurements were made. The dosing time's dependence on the drop size (i.e., the length of the major axis of the ellipsoid) is represented in Figure 4. The drop growth is linear in time and increases at a rate of 1.77 μm/hour. However, there are some drops that are much larger than the mean drop size and can be attributed to coalescence of smaller drops or preferred growth of the drop at a defect site on the mica surface as is shown in Figure 1b. The drop density is linear with $1/r^2$, where r is length of the major axis as is shown in Figure 5. The $1/r^2$ dependence, which follows from the surface area of drop that is in contact with the mica surface, appears to be a reasonable approximation for the drops, although they are slightly ellipsoidal. Also, it is noted that the larger drops (see Figure 1b) have a greater separation distance from neighboring drops. This appears to indicate that some drops do grow by coalescence with one another.

The ellipsoidal shape of the drops may arise from a nonuniform interface between the drop and the mica surface or by a slight tilt in the sample which causes the sample to flow in the direction of the tilt. However, we
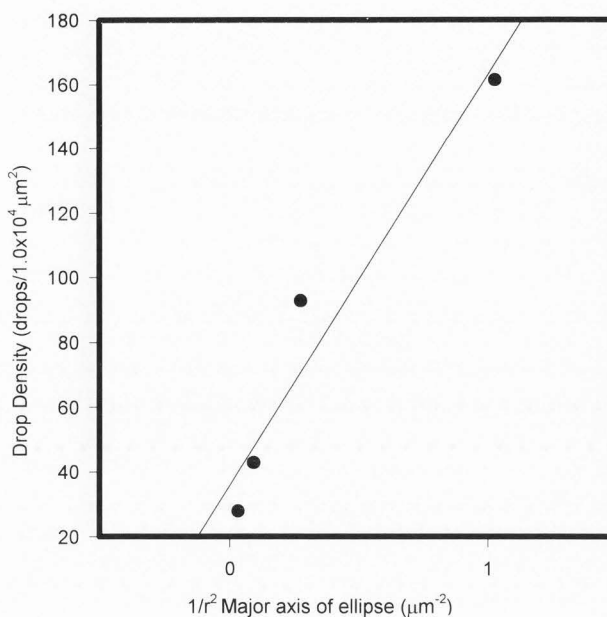
Figure 5. Plot of drop density for dosing times of 1, 2, 4, and 6 hours versus the reciprocal of the square of the mean drop radius.

----

deliberately tilted the sample in several directions, but observed no change in the droplet shape. Apparently, the supercooled droplets are quite viscous and do not show any measurable distortion when the substrate is inclined. We can only suggest at this point that the ellipsoidal shape of the drops may arise from some air-TNT-surface perturbation which allows for the minimum energy of the drop to be an ellipsoid and not a sphere. Occasionally, we do observe steps on the (001) surface, and these steps could induce the ellipsoidal drop shape. Some evidence supporting this hypothesis appears to be indicated in Figure 1b where large drops that have formed on a step are distorted into an ellipsoidal shape. However, further investigations of TNT on highly stepped surfaces and different planes is required to verify this hypothesis.

Several samples showed that the crystallization of TNT after 8 hours of dosing has a preferred direction of growth and an area surrounding the crystallites which is depleted of TNT drops. However, there appears to be no relation between preferred growth direction and the mica lattice. Rather, the elongated crystals are representative of the morphology observed from TNT crystals grown from the melt (Philp and Thorpe, 1976). TNT liquid at room temperature is metastable, and a slight perturbation to the supercooled liquid can trigger its solidification. A mechanism for introducing such an instability can result from a drop which has reached a critical

size and has collapsed due to a surface heterogeneity. Once the drop is broken and begins to spread on the surface, a crystallization front is initiated (Philp and Thorpe, 1976). As the crystallization front grows, it engulfs drops in its path converting them into crystals until no more drops can be engulfed by the crystallization front. The engulfment of drops which are in the path of the crystallization front can account in part for the area depleted of drops as indicated in Figure 1d. Another factor which can contribute to the depletion is the 10% shrinkage TNT undergoes when it transforms from a liquid to a solid (Federoff, 1980). Another contribution to creating the depleted area is the enthalpy of fusion of TNT. The heat of fusion resulting from the solidifying drop/crystal front can cause some of the TNT clusters and small drops to partially or totally vaporize. In principle, for each mole of TNT fused, 0.277 moles could be vaporized (Federoff, 1980) which would certainly result in significant depletion of drops in the region of crystal growth. This is particularly evident in Figure 1e which shows that the drop size increases as the distance from the crystallites increases. This probably corresponds to the thermal gradient produced when the heat wave, resulting from the enthalpy of fusion, propagated along the crystal surface. Consequently, most of the drops are vaporized within ~100 μm of the crystal, and at greater distances, they begin to appear with an average size of 5 μm; they continue to increase to an average stable value of 8 μm.

We suggest that the large circular areas in the AFM image are due to residues of TNT left after the crystallization front engulfed the drops in its path. The fact that the images show depth contrast rather than features above the mica surface is attributed to the torsional action of the AFM tip. This has been observed for various materials that have been imaged by AFM under conditions of high humidity (> 50%). The high humidity causes a large capillary force that leads to warping the cantilever by rotating it in the plane of the scanned direction (Thundat *et al.*, 1992). This results in a higher lateral force; thus scanning in the x-direction, which is parallel to the axis of the cantilever, causes it to buckle, yielding false contrast not directly attributable to z-piezo displacement from the true sample topography.

When sufficiently high lateral forces occur and the x-scan direction is such that it causes the cantilever tip to roll towards the photo-diode, this results in a negative image for features above the plane of the substrate since the beam deflection behaves as if the cantilever is tracing out a depression on the surface. Conversely, when the scan direction is such that the cantilever tip rolls away from the photo-diode, the resulting image appears as a positive contrast feature. The images of the TNT deposited mica shown in Figures 2 and 3 were obtained

with the scan direction going from the right side of the image to the left side. This is the x-scan direction that can lead to reverse contrast with sufficient lateral friction. When examining the AFM images of the large circular regions, it is apparent that the residue remaining on the surface is relatively soft. Also, the lift-off forces measured for the interior of the circle are much larger than those outside the circle. This would indicate the residue inside the circle has a higher adhesion than outside the circular region. Under these conditions, it is likely that the adhesion force between the TNT and the cantilever tip is sufficient to induce an increased lateral force when scanning from the mica onto the large circular features. In Figures 3c and 3d, it was seen that the residue was pushed to one side, revealing the mica substrate under it. When a cross-section is taken across the region that has the pushed residue, it was observed that the mica protruded from the adjacent residue by about 60 nm. This suggests that the material that has the negative contrast is indeed stickier than the underlying mica and is therefore above the plane of the mica surface.

The lift-off forces measured on the residues reveal that those in the interior of the circle have a higher adhesion force than those outside the circle. This would seem to suggest that the material within the circle is softer than the regions outside. Further, this may indicate that different materials are residing in different bonding sites on the mica crystal surface. The small bright particles, average approximately 150 nm in diameter and 10-15 nm high, observed inside and outside the domain of the large circle depicted in the AFM images were never observed on the virgin mica surface, but do appear after dosing with TNT. These particles appear to be more robust and less affected by the cantilever than the large circular regions. It is certainly possible that these particles may be TNT clusters or crystallites that undergo a transition from a liquid phase to solid at favorable, specific bonding sites on the mica. However, it is also conceivable that the small features may be due to residual chemical impurities related to nitrobenzene compounds that are common impurities found in TNT (Philp and Thorpe, 1976).

Conclusions

Both optical microscopy and atomic force microscopy were used to image TNT on a mica (001) surface. The optical studies indicated that TNT resides on the surface as small drops which reach a critical size and then crystallize into platelets. The crystallization front is exothermic and appears to cause nearby drops and clusters of TNT to vaporize. After six hours of dosing the TNT drops appear ellipsoidal. We suggest the ellipsoidal shape may be due to anisotropy in the surface ten-

sion induced by a surface heterogeneity. The AFM measurements reveal regions of residual TNT which are characterized by their lift-off forces. The inherent artefacts for AFM operating in the contact mode employing the light beam deflection method for production of image contrast results in some limitations for this technique. New measurements operating the AFM in the tapping mode as well as using lateral force probe microscopy to image clusters of TNT are currently underway. It would be useful to perform a high resolution scanning probe microscope study of TNT deposited on mica as well as other crystalline surfaces. Such experiments may give insight to the mechanism of TNT adsorption and aggregation on certain crystalline surfaces.

Acknowledgements

References

Federoff BT (1980) Encyclopedia of Explosives and Related Items. Picatinny Arsenal, Dover, New Jersey, pp. T259-T264.

Henderson DO, Silberman E, Chen N, Snyder F (1993) Adsorption kinetics of EGDN on ZnO by diffuse reflectance infrared fourier transform spectroscopy. Appl. Spectros. **47**: 528-532.

Khan SM (1992) Proceedings of the First International Symposium of Explosive Detection Technology. Federal Aviation Administration Technical Center, Atlantic City, New Jersey. pp. 505-617.

Leggett DC (1977) Vapor pressure of 2,4,6-Trinitrotoluene by a gas chromatography headspace technique. J. Chromat. **133**: 83-90.

Pella PA (1977) Vapor pressure and heats of sublimation of some high melting organic explosives. J. Chem. Thermodyn. **9**: 301-305.

Philp DK and Thorpe BW (1976) Nucleation of 2,4,6-trinitrotoluene by 2,2',4,4',6,6'-hexanitrostilbene, J. Non-Cryst. Solids **35**: 133-138

Thundat T, Warmack RJ, Ellison DP, Bottomley LA, Lourenco AJ Ferrell J (1992) Atomic force microscopy of deoxyribonucleic acid strands adsorbed on mica: The effect of humidity on the apparent width and image contrast. J. Vac. Sci. Technol. A **10**: 630-635.

Xu S, Arnsdorf MF (1994) Calibration of the scanning (atomic) force microscope with gold particles. J. Microsc. **173**, 199-210.

Discussion with Reviewers

Reviewer 1: Another explanation for the small "blips"

in the AFM image of Figure 2 is that they are "nanoexplosions" created by friction of the AFM tip scanning along a film of TNT. A statistical study of their height and frequency as a function of loading force might shed some light on this possibility.

Authors: While the idea that the blips in Figure 2a may be attributed to nanoexplosions is interesting, we do not believe that these features are due to nanoexplosions for the following reason: We carried out AFM studies on TNT films where we have used a loading force sufficient to scrape away part of the TNT film on the mica surface and did not observe such blips as in Figure 2a. Clearly, the loading force used to scrape away the TNT (we included representative images in Figures 2b, 2c, 2d, and 2e showing the scraped region) is greater than that used to obtain the image in Figure 2a and, as such, we would expect to see more blips (nanoexplosions). However, because we did not observe the blips with higher loading force, we conclude that these features are not due to nanoexplosions of TNT, but they are more likely due to TNT which nucleated at specific sites on the mica surface. Another possibility is that they may be attributed to nitro-benzene derivatives which are common impurities in TNT that have segregated from TNT during crystallization. At this point, we can not determine if the blips are residual impurities or TNT that nucleated at specific sites, but we can conclude that they are not features that result from nanoexplosions.

Reviewer II: Please comment on the calibration error observed in the AFM image of virgin mica surface, i.e., the lattice spacing is not consistent in all three symmetry directions. The lateral calibration problem invalidates the authors statement that they observed particles 0.17 μm in diameter.

Authors: The problem observed in the lateral calibration for the (001) mica surface resulted from measurements made with a 0.4 μm scanner. All other measurements for TNT adsorbed on mica were made with a 12 μm scanner which was calibrated using a standard gold grid with 1 μm spacings supplied by Digital Instruments. Consequently, the image of the mica surface recorded with the 0.4 μm scanner and the associated lateral calibration problem is not relevant to the images recorded with the 12 μm scanner. For this reason, we have deleted this figure from the manuscript. Regarding the error in the 0.17 μm size particles, we agree that there is indeed error in the particle size, but it not possible to extrapolate the error observed in the atomically resolved mica image to 0.17 μm particles. In fact, it has been established that calibration of the AFM tip with mica provides little clue as to type of distortion and the amount of lateral broadening observed when larger particles are scanned (Xu and Arnsdorf, 1994). Thus, we

only use the dimension of 0.17 μm to refer to the object in the figure, and not as a measure of the particle size.

G.W. Zajac: The small 0.1-0.2 μm features of high contrast in Figure 2 believed to be residue of TNT are of interest. Did the authors image these regions in higher magnification by AFM, and can they elaborate on any results about these smaller regions? The scanning probes excel at inspecting such microscopic features. One possibility is that these are microscopic TNT crystallites. Would the authors care to discuss this?

Authors: We did not measure the small 0.1-0.2 μm features at higher magnification. The fact that they appear to be more robust and less affected by the cantilever than the circular regions may suggest that they may be due nitro-benzene related materials which are commonly found in TNT. Alternatively, they may be TNT nanocrystals as you suggest, which have nucleated at certain sites on the mica surface. However, we can not at this point determine if the material is or is not TNT based on only the AFM measurements. Measuring the Raman spectrum with a microprobe focused on the small feature or the infrared spectra with a microscope focused on the small 0.1-0.2 μm features would certainly help in identifying their composition.

R. Balhorn: Can one estimate the range in distance over which the enthalpy of fusion should have an impact on the drops? It would be nice to see if it fits with what is observed.

Authors: It is possible to model this type of a problem by solving a two-dimensional differential equation of heat diffusion. The following assumptions can be made: (1) the heat Q evolved during solidification is instantaneous since the drops are supercooled by 58°C at room temperature, (2) the heat source Q is a line source at x_0 = z_0 = 0 and is not a function of time.

Due to the fact that the thermal conductivity of mica is anisotropic, the conductivity along the Z direction perpendicular to the layer (x and y) is 17 times smaller than along the x and y direction. Therefore, a one-dimensional heat diffusion is a reasonable approximation to the problem. The one-dimensional Greens function is given as

$$G(x, x_o, t, t_o) = [(1/2\pi^{1/2}) \{1/(D^2)(t-t_o)^{1/2}\} \exp^{-\{(x-x_o)/2D)\}^2}] \quad (1)$$

The temperature profile can be obtained by the integral

$$T(x,t) = \{1/(C_p\rho)\} \int_0^\infty Q(0,0) \, G(x, x_o, t, t_o) \, dx \, dt \quad (2)$$

In equations (1) and (2), D is thermal diffusivity, t is the time after the heat Q evolved at $t_0 = 0$, x is the distance from the source ($x_0 = 0$), Q is the total amount of heat of fusion released upon TNT solidification. Unfortunately, a true temperature profile can not be generated because we are not able to estimate the total mass of TNT that solidified. However, more experiments are planned which will allow for a more quantitative analysis of the heat diffusion problem.